

Z BOSON ASYMMETRY MEASUREMENTS AT THE TEVATRON

B. QUINN

for the CDF and D0 Collaborations

Department of Physics and Astronomy, University of Mississippi, University, MS 38677, USA

We present measurements of the forward-backward asymmetry (A_{FB}) in dilepton pair decays of Z bosons produced in $p\bar{p}$ collisions using the full Tevatron dataset. The CDF experiment extracts a value for the effective weak mixing angle parameter $\sin^2\theta_{eff}^l$ of 0.2315 ± 0.0010 from the A_{FB} distribution of dimuon events in 9.2 fb^{-1} of integrated luminosity. From dielectron events in 9.7 fb^{-1} of data, the D0 experiment finds $\sin^2\theta_{eff}^l = 0.23106 \pm 0.00053$, the world's most precise measurement of $\sin^2\theta_{eff}^l$ from hadron colliders and with light quark couplings.

1 Introduction

Drell-Yan lepton pairs¹ are produced at the Tevatron through the reaction

$$p\bar{p} \rightarrow Z/\gamma^* \rightarrow \ell^+ \ell^- \quad (1)$$

at $\sqrt{s} = 1.96 \text{ TeV}$. The angular distribution of these pairs is sensitive to the weak mixing angle through the vector coupling to the Z boson, $g_V^f = I_3 - 2Q_f \sin^2\theta_W$. This coupling is altered by weak radiative corrections of a few percent to give an effective weak mixing parameter, $\sin^2\theta_{eff}^l$.

The angular distribution is measured in the Collins-Soper rest frame of the Z , in which θ^* is defined as the angle of the ℓ^- relative to the direction of the incoming quark.² Events are categorized as forward (backward) if $\cos\theta^* \geq 0$ ($\cos\theta^* < 0$). After integrating over the azimuthal angle, the next to leading order QCD expression for the angular distribution becomes³

$$dN/d\Omega \propto 1 + \cos^2\theta^* + A_4 \cos\theta^*. \quad (2)$$

The forward-backward asymmetry is

$$A_{FB} = \frac{\sigma^+ - \sigma^-}{\sigma^+ + \sigma^-} = \frac{3}{8}A_4, \quad (3)$$

where σ^+ and σ^- are the forward and backward cross sections, respectively, and the A_4 parity violating term is sensitive to the weak mixing angle through Z self-interference.

Both the CDF⁴ and D0⁵ experiments employ general, multi-purpose detectors featuring excellent central tracking, calorimeter, and muon identification systems particularly relevant to these analyses and described in detail elsewhere. CDF has recently published a measurement of $\sin^2\theta_{eff}^l$ from A_{FB} in dimuon events.⁶ D0 has a new preliminary $\sin^2\theta_{eff}^l$ result in the dielectron channel.⁷ Both analyses are carried out in four steps: measure A_{FB} from dilepton events in bins of dilepton invariant mass (M), produce Monte Carlo (MC) templates of $A_{FB}(M, \sin^2\theta_W)$, perform full corrections to data and simulation, and extract $\sin^2\theta_{eff}^l$ by doing a χ^2 comparison between the data and MC.

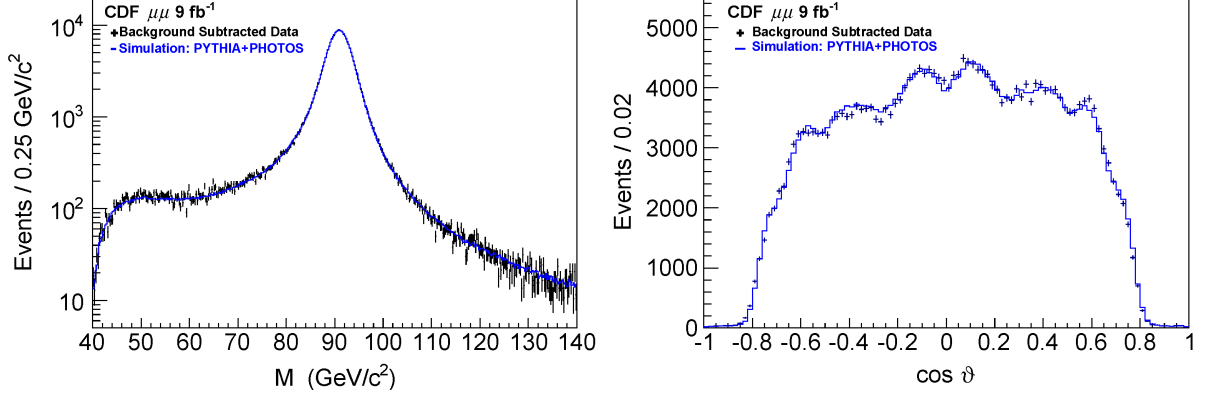


Figure 1 – CDF dimuon invariant mass (left) and Collins-Soper frame $\cos \theta^*$ (right) distributions.

2 CDF: $\sin^2 \theta_{eff}^l$ from dimuon events

CDF collected a sample of dimuon Drell-Yan pairs from the full dataset comprising 9.2 fb^{-1} of integrated luminosity. Selection cuts on the muons included the transverse momentum and rapidity requirements $p_T > 20 \text{ GeV}$ and $|y| < 1$, respectively, as well as $M > 50 \text{ GeV}$. A key part of the analysis is a very precise momentum calibration using a method that tunes the data and simulation to post-final state radiation (FSR) generator level distributions in 64 individually calibrated bins of pseudorapidity and azimuthal angle. Dimuon events with eleven different muon subdetector topologies of muon location were included in the sample. Backgrounds from electroweak sources ($WW, WZ, ZZ, t\bar{t}, W+\text{jets}, Z \rightarrow \tau^+\tau^-$) are estimated from MC to be 0.53%. QCD backgrounds are determined from data to be a negligible 0.10%. MC simulations were PYTHIA-based,⁸ using CTEQ5L⁹ parton distribution functions (PDFs) and a GEANT¹⁰ simulation of the CDF detector. After background subtraction, 276,623 events remained in the dimuon sample. The data and MC distributions of M and $\cos \theta^*$ in the final sample are shown in Fig. 1.

For this analysis, a traditional asymmetry measurement applying efficiency \times acceptance corrections to calculate cross sections (e.g. $\sigma^+ = N^+ / (\epsilon A)^+$) would be quite challenging. It would require 22 correction numbers for the 11 different muon topologies, resulting in statistical limitations from this subdivision of the data sample. An alternative event weighting method¹¹ is employed which is equivalent to measuring A_{FB} in bins of $\cos \theta^*$. The asymmetry is calculated according to

$$A_{FB}(|\cos \theta^*|) = \frac{A_{FB}|\cos \theta^*|}{1 + \cos^2 \theta^* + \dots}, \quad (4)$$

assuming local ϵA equivalence for forward and backward events and NLO QCD angular distribution. This angular weighting results in more accurate measurements in bins of large $\cos \theta^*$. The binned measurements are then recast into an unbinned weighted event sum

$$A_{FB} = \frac{N_n^+ - N_n^-}{N_d^+ + N_d^-}, \quad (5)$$

where the n, d subscripts refer to numerator and denominator event weights which remove the angular dependencies from Eq. 4 while preserving measurement accuracy at each $\cos \theta^*$. This is equivalent to performing a maximum likelihood fit, and delivers an expected 20% reduction in uncertainty. The raw A_{FB} distribution seen in Fig. 2(left) must then be unfolded to correct for resolution smearing and QED FSR effects. Final bin-by-bin 2^{nd} order bias corrections are then applied to account for limited rapidity coverage and detector non-uniformities, yielding the fully corrected A_{FB} distribution shown in Fig. 2(right).

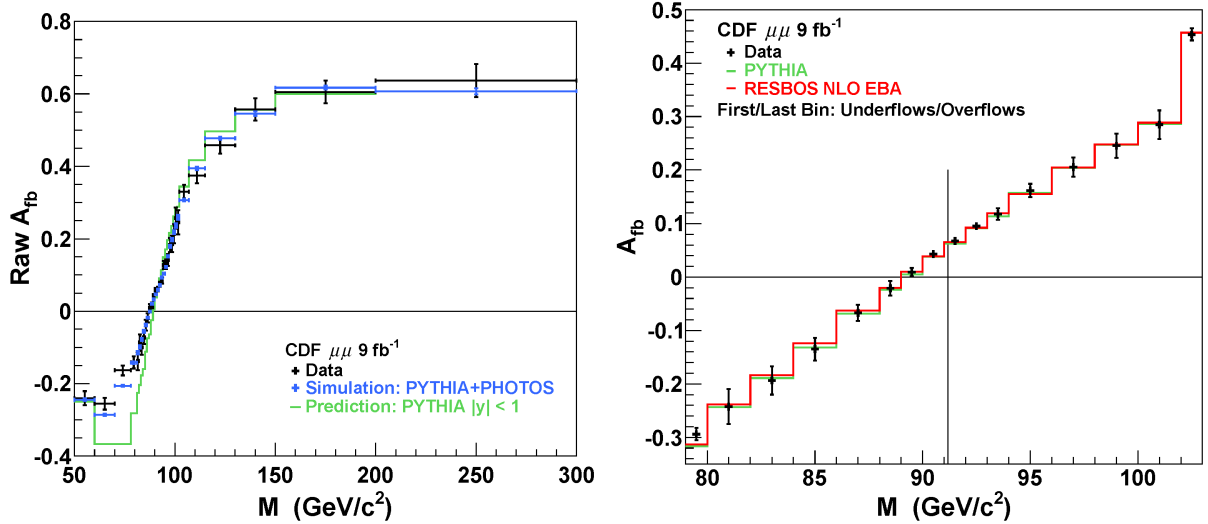


Figure 2 – CDF raw A_{FB} (left) and fully corrected A_{FB} (right) distributions.

The A_{FB} measurement is then compared to A_{FB} templates calculated at different values of $\sin^2\theta_W$. Three sets of templates are used, each with a different Enhanced Born Approximation (EBA) calculation (NLO RESBOS¹², NLO POWHEG-BOX¹³, and LO tree), and all producing consistent results. The RESBOS comparison gives the smallest χ^2 and is selected as the default template set. The dominant systematic uncertainty comes from the PDF uncertainty. Smaller uncertainties include those on EBA calculation, backgrounds, and momentum and QCD scales. All systematic uncertainties are much smaller than the statistical uncertainty of the measurement. The χ^2 fit to the RESBOS templates gives the value $\sin^2\theta_{eff}^l = 0.2315 \pm 0.0009_{stat} \pm 0.0004_{syst}$. Using an on-shell renormalization scheme in a Standard Model (SM) context, this result is converted to $\sin^2\theta_W = 0.2233 \pm 0.0008_{stat} \pm 0.0004_{syst}$, from which is obtained an indirect measurement of the W boson mass, $M_W = 80.365 \pm 0.043_{stat} \pm 0.019_{syst}$.

3 D0: $\sin^2\theta_{eff}^l$ from dielectron events

Dielectron events were selected from D0's full dataset of 9.7 fb^{-1} . Electrons found in the central (CC) and endcap (EC) calorimeters with $p_T > 25 \text{ GeV}$ and $M > 50 \text{ GeV}$ were accepted. Compared to the previous D0 5 fb^{-1} publication,¹⁴ an increase in statistics 85% beyond luminosity scaling was achieved by extending the pseudorapidity range to $|\eta| < 1$ and $1.5 < |\eta| < 3.2$, including events with both electrons in the endcaps and those with electrons near calorimeter module boundaries, and improving track reconstruction. The final sample consisted of 560,267 events with low QCD and negligible electroweak backgrounds totaling 0.4% for central and $< 4\%$ for endcap events. The MC samples were generated with PYTHIA⁸ using CTEQ6L1¹⁵ PDFs and a GEANT-based¹⁰ simulation of the D0 detector.

Electron reconstruction in the calorimeters depends critically on the electron energy calibration. The global energy scale modeling used in the previous D0 analysis is inadequate for the current measurement because shape dependencies of the different detector responses over the extended acceptance regions are too great. A new method was developed that corrects energy as a function of instantaneous luminosity (L_{inst}) first, and then as a function of detector pseudorapidity (η_{det}). This procedure scales the Z mass peak to the LEP value of 91.1875 GeV in each (L_{inst}, η_{det}) bin. Calibrations are performed separately for data and MC. After calibration, the mass peak dependence on L_{inst} is negligible, and the dependence on η_{det} is reduced from 2 GeV to 100 MeV for data and 10 MeV for MC. The improvement of η_{det} dependence in data is illustrated in Fig. 3. Energy resolution and efficiency corrections are applied, and reweightings particularly as functions of L_{inst} and vertex z are performed. Final distributions of M and $\cos\theta^*$

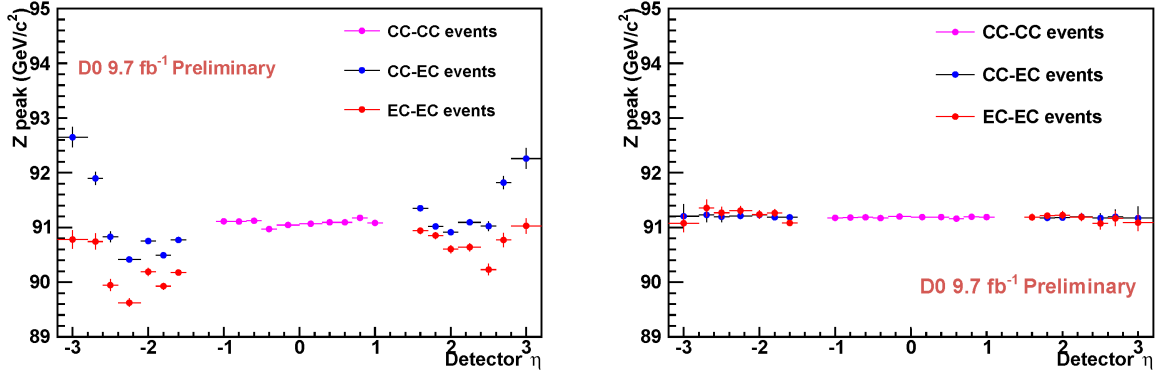


Figure 3 – D0 comparison of Z mass peak position as a function of detector pseudorapidity before (left) and after (right) binned energy scale calibration.

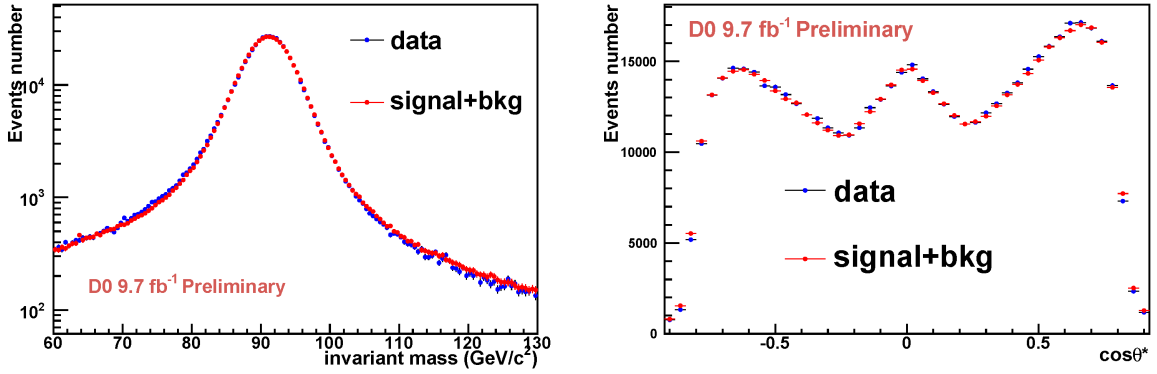


Figure 4 – D0 dielectron invariant mass (left) and Collins-Soper frame $\cos \theta^*$ (right) distributions.

for data and MC are displayed in Fig. 4.

The $\sin^2 \theta_{eff}^l$ extraction is performed separately for subsamples based on location of the two electrons (CC-CC, CC-EC, EC-EC), and on run period (RunIIa: 1.1 fb^{-1} low L_{inst} , RunIIb: 8.6 fb^{-1} high L_{inst}). The full dataset distributions of A_{FB} for all three event topologies can be seen in Fig. 5. Determination of $\sin^2 \theta_{eff}^l$ is made through χ^2 comparisons of these distributions with MC templates generated at different values of $\sin^2 \theta_W$ by reweighting the generator level ($M_{Z/\gamma^*}, \cos \theta^*$) distribution from the default MC ($\sin^2 \theta_W = 0.232$). The PDF uncertainty is the dominant systematic uncertainty in this analysis, with smaller contributions from energy scale and smearing, charge and electron misidentification, and backgrounds. The extracted value of $\sin^2 \theta_W$ is $0.23098 \pm 0.00042_{stat} \pm 0.00014_{syst} \pm 0.00029_{PDF}$. In a SM context with on-shell renormalization scheme and RESBOS EBA correction, this corresponds to $\sin^2 \theta_{eff}^l = 0.23106 \pm 0.00053$. This is the most precise determination of $\sin^2 \theta_{eff}^l$ from a hadron collider and from light quark couplings.

4 Conclusions

We report two new measurements of $\sin^2 \theta_{eff}^l$ from the forward-backward asymmetry of Drell-Yan pairs at the Tevatron. CDF finds a value of $\sin^2 \theta_{eff}^l = 0.2315 \pm 0.0010$ from studies of dimuon events, and D0 obtains a preliminary result of $\sin^2 \theta_{eff}^l = 0.23106 \pm 0.00053$ from a sample of dielectron events. Both results are compared to and shown to be consistent with previous determinations of $\sin^2 \theta_{eff}^l$ from the LEP and SLD Collaborations in Fig. 6.¹⁶

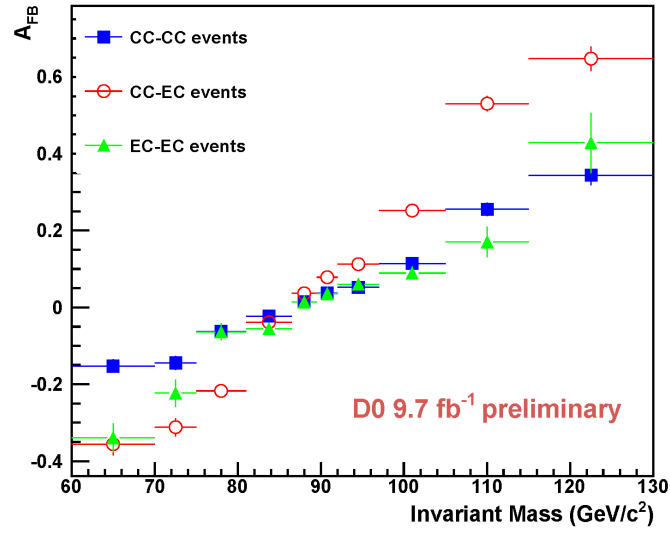


Figure 5 – D0 A_{FB} distributions for all three dielectron event topologies.

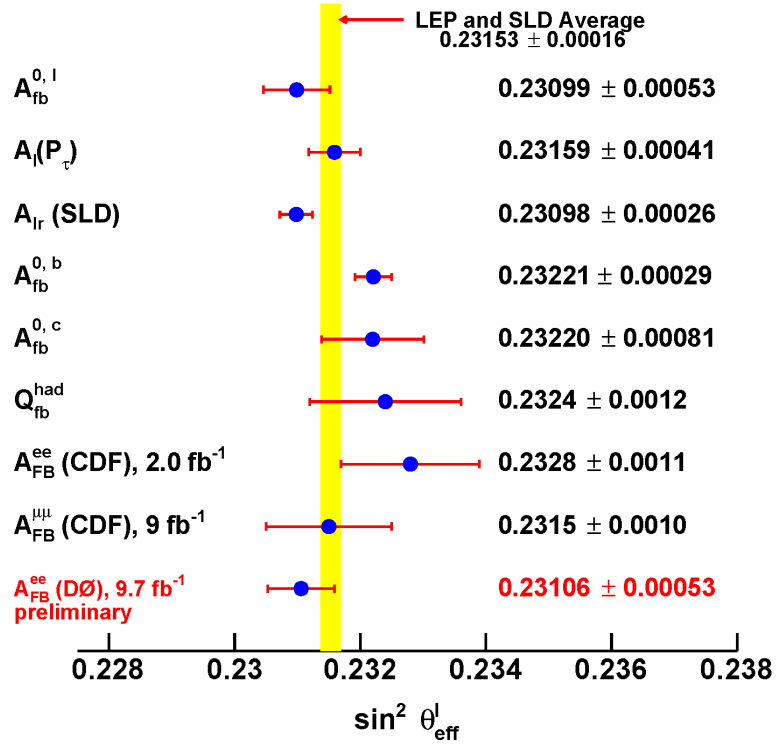


Figure 6 – Comparison of Tevatron $\sin^2 \theta_{eff}^l$ results with those from LEP and SLD experiments.

References

1. S.D. Drell and T.-M. Yan, *Phys. Rev. Lett.* **25**, 316 (1970).
2. J.C. Collins and D.E. Soper, *Phys. Rev. D* **16**, 2219 (1977).
3. E. Mirkes, *Nucl. Phys. B* **387**, 3 (1992); E. Mirkes and J. Ohnemus, *Phys. Rev. D* **50**, 5692 (1994).
4. T. Aaltonen *et al* (CDF Collaboration), *Phys. Rev. D* **85**, 012009 (2012).
5. V.M. Abazov *et al* (D0 Collaboration), *Nucl. Instrum. Methods* **565**, 463 (2006); M. Abolins *et al*, *Nucl. Instrum. Methods* **584**, 75 (2008); R. Angstadt *et al*, *Nucl. Instrum. Methods* **622**, 298 (2010).
6. T. Aaltonen *et al* (CDF Collaboration), *Phys. Rev. D* **89**, 072005 (2014).
7. S. Yang *et al* (D0 Collaboration), D0 Note 6426-CONF 2014.
8. T. Sjöstrand *et al*, *Comp. Phys. Commun.* **135**, 238 (2001).
9. H.L. Lai *et al* (CTEQ Collaboration), *Eur. Phys. J. C* **12**, 375 (2000).
10. R. Brun and F. Carminati, CERN Program Library Long Writeup W5013, 1993 (unpublished).
11. A. Bodek, *Eur. Phys. J. C* **67**, 321 (2010).
12. G.A. Ladinsky and C.-P. Yuan, *Phys. Rev. D* **50**, R4239 (1994); C. Balazas and C.-P. Yuan, *Phys. Rev. D* **56**, 5558 (1997); F. Landry *et al*, *Phys. Rev. D* **67**, 073016 (2003); A. Konychev and P. Nadolsky, *Phys. Lett. B* **633**, 710 (2006).
13. S. Alioli *et al*, *J. High Energy Phys.* **07**, 060 (2008).
14. V.M. Abazov *et al* (D0 Collaboration), *Phys. Rev. D* **84**, 012007 (2011).
15. J. Pumplin *et al*, *J. High Energy Phys.* **07**, 012 (2002); D. Stump *et al*, *J. High Energy Phys.* **10**, 046 (2003).
16. G. Abbiendi *et al* (LEP Collaborations ALEPH, DELPHI, L3 and OPAL; SLD Collaborations; LEP Electroweak Working Group; SLD Electroweak and Heavy Flavor Groups), *Phys. Rep.* **427**, 257 (2006).
17. C Jarlskog in *CP Violation*, ed. C Jarlskog (World Scientific, Singapore, 1988).
18. L. Maiani, *Phys. Lett. B* **62**, 183 (1976).
19. J.D. Bjorken and I. Dunietz, *Phys. Rev. D* **36**, 2109 (1987).
20. C.D. Buchanan *et al*, *Phys. Rev. D* **45**, 4088 (1992).